ScienSage

Journal of Advanced Scientific Research

Available online through http://www.sciensage.info/jasr

ISSN
0976-9595
Research Article

DFT AND VIBRATIONAL SPECTROSCOPIC STUDY ON PYRIMIDINE DERIVATIVE INSECTICIDE

Laila Stephenson Anju[1], Devadhas Aruldhas[2]*

[1]*Research Scholar, Reg. Number: 12049, Manonmaniam Sundaranar University, Abishekapatti, Tirunelveli, Tamil Nadu, India.*

[2]*Department of Physics& Research Centre, Nesamony Memorial Christian College,Marthandam Tamilnadu, India.*

**Corresponding author: anju.ls2007@gmail.com*

ABSTRACT

A complete vibrational analysis of (6-methyl-2-thiophen-2-ylpyrimidin-4-yl) *N*,*N*-dimethylcarbamate (MTPD) was performed by using theoretical information using density functional theory based on scaled quantum chemical approach. The structural and spectroscopic data of the molecule were obtained from B3LYP with 6-31G(d) basis set calculations. The complete vibrational distributions were performed on the basis of the potential energy distribution (PED) of the vibrational energy distribution analysis (VEDA 4) program. The stable geometry of the compound has been determined from potential energy surface scan. The calculated HOMO and LUMO energies show that charge transfer occur within the molecule. Comparison of simulated spectra with the experimental spectra provides important information about the ability of the computational method to describe the modes of vibration. Natural charge analysis and molecular electrostatic potential (MESP) has been calculated.

Keywords: Pyrimidine, Vibrational analysis, reactivity, UCA Fukui, MESP

1. INTRODUCTION

Pyrimidine represents one of the most active classes of compounds, possessing a wide spectrum of biological activity [1]. It belongs to the family of nucleic acids and is of great interest, since they control the manufacture of protein and the functions of cell in living organisms. Pyrimidine does not exist in nature but in the form of its different derivatives are found as a part of more complex systems and are widely distributed. Pyrimidine and its derivatives are known for their biological activity and have related much attention from spectroscopists, drug, clinical and industrial researchers because of their therapeutic importance [2]. Nitrogen containing cyclic compounds has been increasing interest because of their utility in various applications. They are present in wide variety of drugs, biologically active compounds including insecticidal agents [3]. The current study is to focus on the significance of pyrimidine and its derivative as insecticidal agents to the development of more potent and effective insecticidal agents.

In the present study the molecular structure of (6-methyl-2-thiophen-2-ylpyrimidin-4-yl) *N*,*N*-dimethyl -carbamate (MTPD) is described. The purpose of this work is to investigate the performance of DFT method in predicting geometry and vibrational spectra of the title compound. The natural bond orbital (NBO) analysis, Molecular electrostatic potential should help us to understand the structural and spectral characteristics and bioactivity of the compound.

2. MATERIALS AND METHODS

All geometric structure calculation have been carried out using Gaussian 09 package and and Gauss view molecular visualizing program package, which has provided itself to be extremely useful to get a clear knowledge of optimized parameters, vibrational wavenumber, electronic structure properties and other molecular properties [4]. The geometry is fully optimized at Beck 3-Lee-Yang-Parr (B3LYP) level with standard 6-31G(d) basis set [5]. The computed wavenumbers were scaled by 0.9614 [6]. Additionally the calculated vibrational frequencies are clarified by means of the Potential energy distribution (PED) analysis of all fundamental vibrational modes by using Veda.4 program [7]. The theoretical tool Fukui function was performed by UCA-FUKUI software to understand the chemical reactivity the condensed Fukui function and related local and global parameters are calculated [8]. Potential Energy scan (PES) was performed to obtain a stable geometry of the compound.

3. RESULTS AND DISCUSSION

3.1. Molecular Geometry

Complete geometrical parameters were performed within the C_1 point group symmetry for the title compound (MTPD), the optimized geometries are shown in fig. 1 and are listed in table 1. The optimized structure parameters (bond length, bond angle, dihedral angle) of TMPD was calculated at DFT B3LYP/6-31G(d) basis set. The optimized geometries give nearly non planar structure to the compound. The backbone of the MTPD molecule consists of one methyl pyrimidine and a dimethyl carbamate.

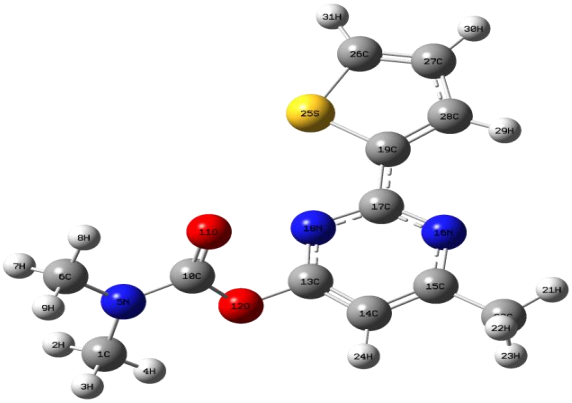

Fig. 1: Optimized structure of MTPD

Table 1: Optimized structure parameters of MTPD

Bond Length	Exp. value	Calculated value	Bond Angle	Exp. value	Calculated value	Dihedral angle	Exp. value	Calculated value
(A^0)			(^{0})			(^{0})		
C_1-H_2	0.98	1.098	H_2-C_1-H_3	109.5	108.1	H_2-C_1-N_5-$_{C6}$	69.3	55.6
C_1-H_3	0.98	1.098	H_2-C_1-H_4	109.5	109	H_2-C_1-N_5-C_{10}	-104.9	-122.3
C_1-H_4	0.98	1.087	H_2-C_1-N_5	109.4	110.7	H_3-C_1-N_5-C_6	-50.8	-63.6
C_1-N_5	1.456	1.455	H_3-C_1-H_4	109.5	109	C_3-C_1-N_5-C_{10}	-104.9	118.4
N_5-C_6	1.457	1.455	H_3-C_1-N_5	109.5	109.7	H_4-C_1-N_5-C_6	-170.7	175.8
N_5-C_{10}	1.337	1.361	H_4-C_1-N_5	109.5	110.3	H_4-C_1-N_5-C_{10}	15.1	-2.2
C_6-H_7	0.98	1.098	C_1-N_5-C_6	117.1	116.5	C_1-N_5-C_6-H_7	55.2	-61.7
C_6-H_8	0.98	1.089	C_1-N_5-C_{10}	124.9	125.1	C_1-N_5-C_6-H_8	175.2	178.3
C_6-H_9	0.98	1.098	C_6-N_5-C_{10}	117.9	118.4	C_1-N_5-C_6-H_9	55.2	58.1
C_{10}-O_{11}	1.213	1.211	N_5-C_6-H_7	109.5	110.3	C_{10}-N_5-C_6-H_7	-130.2	116.4
C_{10}-O_{12}	1.37	1.399	N_5-C_6-H_8	109.5	108.9	C_{10}-N_5-C_6-H_8	-10.24	-3.6
O_{12}-C_{13}	1.398	1.373	N_5-C_6-H_9	109.5	110.4	C_{10}-N_5-C_6-H_9	109.7	-123.8
C_{13}-C_{14}	1.382	1.394	H_7-C_6-H_8	109.5	109.4	C_1-N_5-C_{10}-O_{11}	176.8	176.1
C_{13}-N_{18}	1.314	1.321	H_7-C_6-H_9	109.5	108.4	C_1-N_5-C_{10}-O_{12}	-4.0	-7.5
C_{14}-C_{15}	1.401	1.397	H_8-C_6-H_9	109.5	109.5	C_6-N_5-C_{10}-O_{11}	2.7	-1.8
C_{14}-C_{24}	1.512	1.083	N_5-C_{10}-O_{11}	126.2	126.4	C_6-N_5-C_{10}-O_{12}	-178.1	174.6
C_{15}-N_{16}	1.333	1.342	N_5-O_{10}-O_{12}	111.5	110.6	N_5-C_{10}-O_{12}-C_{13}	176.0	154.6
C_{15}-C_{20}	1.501	1.506	O_{11}-C_{10}-O_{12}	122.3	122.9	O_{11}-C_{10}-O_{12}-C_{13}	-4.8	-28.8
N_{16}-C_{17}	1.345	1.342	C_{10}-O_{12}-C_{13}	115.2	118.4	C_{10}-O_{12}-C_{13}-C_{14}	87.0	132.2
C_{17}-N_{18}	1.351	1.348	O_{12}-C_{13}-C_{14}	119.2	117.9	C_{10}-O_{12}-C_{13}-N_{18}	-95.7	-52
C_{20}-H_{21}	0.98	1.096	O_{12}-C_{13}-N_{18}	114	118.3	O_{12}-C_{13}-C_{14}-C_{15}	175.7	175.9
C_{20}-H_{22}	0.98	1.096	C_{14}-C_{13}-N_{18}	126.8	123.7	O_{12}-C_{13}-C_{14}-C_{24}	-4.2	-4.5
C_{20}-H_{23}	0.981	1.094	C_{13}-C_{14}-C_{15}	113.4	116.1	N_{18}-C_{13}-C_{14}-C_{15}	-1.1	0.3
			C_{14}-C_{15}-N_{16}	122.7	121.4	N_{18}-C_{13}-C_{14}-C_{24}	178.9	179.9
			C_{14}-C_{15}-C_{20}	121.6	122	O_{12}-C_{13}-N_{18}-C_{17}	-177.0	-176.5
			N_{16}-C_{15}-C_{20}	115.8	116.6	C_{14}-C_{13}-N_{18}-C_{17}	-0.02	-0.9
			C_{15}-N_{16}-C_{17}	117.4	116.6	C_{13}-C_{14}-C_{15}-N_{16}	1	0.4
			N_{16}-C_{17}-N_{18}	125	127	C_{13}-C_{14}-C_{15}-C_{20}	-179.0	179.9
			C_{13}-N_{18}-C_{17}	114.7	115.3	C_{14}-C_{15}-C_{20}-H_{21}	-163.3	123.1
			C_{15}-C_{20}-H_{21}	109.5	110	C_{14}-C_{15}-C_{20}-H_{22}	-43.2	-119.2

Continued…

	C_{15}-C_{20}-H_{22}	109.5	111.8	C_{14}-C_{15}-C_{20}-H_{23}	76.8	1.9
	C_{15}-C_{20}-H_{23}	109.4	110	N_{16}-C_{15}-C_{20}-H_{21}	16.8	-57.3
	H_{21}-C_{20}-H_{22}	109.5	109	N_{16}-C_{15}-C_{20}-H_{22}	136.8	60.4
	H_{21}-C_{20}-H_{23}	109.5	107	N_{16}-C_{15}-C_{20}-H_{23}	-103.2	-178.6
	H_{22}-C_{20}-H_{23}	109.5	108.9	C_{15}-N_{16}-C_{17}-N_{18}	-1.6	-0.5
				N_{16}-C_{17}-N_{18}-C_{13}	1.5	1.1
				C_{14}-C_{15}-N_{16}-C_{17}	0.3	-0.3
				C_{20}-C_{15}-N_{16}-C_{17}	-179.8	-179.8

Pyrimidine ring is found to be near planar within small twist exo C_{13}, C_{17}, C_{15} bond angles (N_{18}-C_{13}-O_{12}, O_{20}-C_{13}-C_{14}, N_{16}-C_{17}-S_{19}, C_{14}-C_{15}-N_{16}, C_{14}-C_{15}-C_{20}) notably deviate from the expected triagonal angle and so transfer of electrons is possible between the pyrimidine ring and side chain atoms and this results in the molecular crowding effect arising from steric requirements which is responsible for biological activity. Decrease the endo cyclic angles of C_{13}-N_{18}-C_{17}, C_{13}-C_{14}-C_{15}, C_{15}-N_{16}-C_{17} and the corresponding increase in the endo cyclic angles N_{14}-C_{13}-N_{18}, N_{16}-C_{15}-C_{14}, N_{16}-C_{17}-N_{18} are due to the negative inductive effect in the pyrimidine ring. Lowering of bond angles N_5-C_{10}-O_{12} and C_{10}-O_{12}-C_{13} is due to the charge transfer from pyrimidine ring through carbamate group to the thiophene ring. In the molecule, the dimethyl carbamate part C-H, C-N, C-O, C-C bond lengths are almost identical. But when compared the C_{13}-C_{18} bond length is slightly decreased and C_{16}-C_{17} and C_{18}-C_{17} bond length is increased due to the attachment of thiophene ring. The C_{16}-C_{17}-N_{18} bond angle is calculated in MTPD as 125.8 A°. This is difference is due to the attachment of thiophene groups. This also clears the C_{13}-N_{18}-C_{17} bond angle (116.0 A°).

3.2. NBO Analysis

NBO analysis gives the role of intermolecular hydrogen bonding interaction in the compound. This is carried out by considering all possible interaction between filled donor and empty acceptor. For each donor (i) and acceptor (j), the stabilization energy (E^2) associated with the delocalization i⟶j is determined as

$$E^2 = \Delta Eij = qi(Fi,j)2 \Big/ Ej - Ei$$

Where, q_i is donor orbital occupancy, E_i,E_j are the diagonal elements, F_{ij} is the off diagonal NBO fock matrix element.

Table 2: Possible Hydrogen bonding and hyper-conjugative interactions for MTPD

	Donor	ED (e)	Accepter	ED (e)	E^2 (kJ/mol)
Hydrogen bonding	n_1(O11)	1.815	σ*(C6-H8)	0.009	4.226
		-0.239		0.471	
	n_1(O12)	1.935	σ*(C1-H4)	0.007	3.18
		-0.557		0.462	
	n1(N5)	1.688	σ*(C1-H2)	0.015	18.995
		-0.247		0.433	
Hyperconjugation	n1(N5)	1.688	σ*(C1-H3)	0.016	21.84
		-0.247		0.432	
	n1(N5)	1.688	σ*(C6-H7)	0.014	21.004
		-0.247		0.437	
	n1(N5)	1.688	σ*(C6-H9)	0.014	18.702
		-0.247		0.436	

Table 2 shows the most relevant hydrogen bonding and hyper-conjugative interactions for the compound performed by NBO analysis. The hyper-conjugative interactions are formed by the orbital overlap between σ bond orbital to σ*anti-bonding orbital, which results in intramolecular charge transfer causing the stabilization of

the system. These interactions can be identified by finding the increase in electron density in the anti-bonding orbital.

C-H…O intramolecular hydrogen bonds are possible in MTPD. C_1…O_{12} and C_6…O_{11} distance 2.702 A °and 2.789 A° which are shorter than the sum of related vander Walls radii. The corresponding C-H-O angle is 104.2 A°.

3.3. MESP Analysis

Molecular electrostatic potential represents a point in the space around the molecule to provide an indication of net electrostatic effect produced at the point by the total charge distribution of the molecule and correlate with dipole moment and chemical reactions. The MSEP has been employed as an informative tool of chemistry to describe different physical and chemical features including non-covalent interactions in complex biological system. The Molecular Electrostatic Potential (MESP) is the most useful electrostatic property to study the relation between structure and activity. The molecular electrostatic potential at the surface are presented by distant colours. Red represents the region of most electronegative electrostatic potential. Blue represent the region of the most positive electrostatic potential. Green represents place of zero potential, potential increases in the order red< orange<green<blue. The red region refers to the area would favour interaction and lone pair region predicting site of hydrogen bonding donor. The computed molecular electrostatic potential for MTPD is shown in fig 2. The carbonyl group shows the negative potential or donor nature. This gives the evidence for the possibility of C-H…O hydrogen bonding.

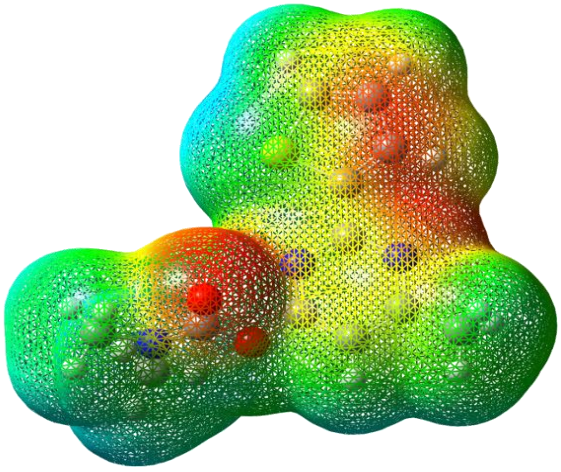

Fig. 2: Molecular electrostatic potential for MTPD

3.4. PES Analysis

A detailed potential energy surface (PES) scan study on dihedral angles N_{16}-C_{15}-C_{20}-H_{21} (φ_1) and H_2-C_1-N_5-C_6 (φ_2) have been performed at B3LYP/6-31G(d) level. The PES scans were carried out by minimizing the potential energy in all geometrical parameters by changing the torsion angle at every 10° for a 360° rotation around the bond. The PES scan are shown in fig 3 .In both the rotations minimum energy is obtained at 60°, 10° and 300°. For φ_1 the minimum energy obtained at 60° is due to the steric interaction H_{23}…H_{24} (2.472 A°) where the stability is increased. The maximum energy is obtained at 360° due to the C_{20}-H_{21}…N_{16} interaction (H_{21}…N_{16} = 2.714 A°).

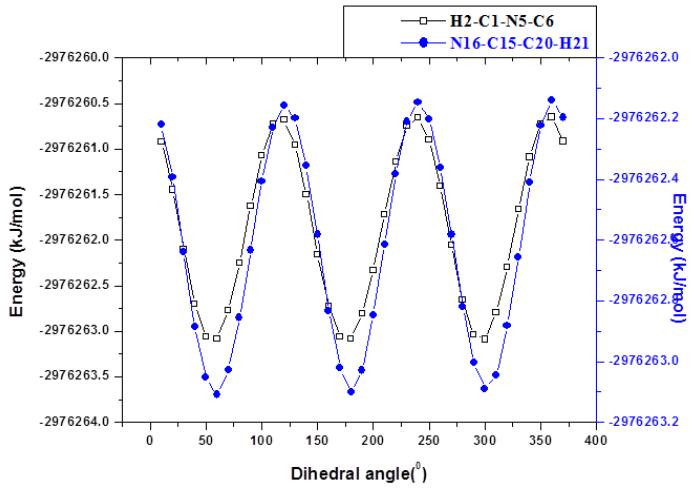

Fig. 3: Potential energy Scan curve of MTPD

3.5. Charge Analysis

The natural charge of title compound is shown in Fig 4. The result shows that the substitution of thiophene ring by pyrimidine ring leads to the redistribution of electron density.

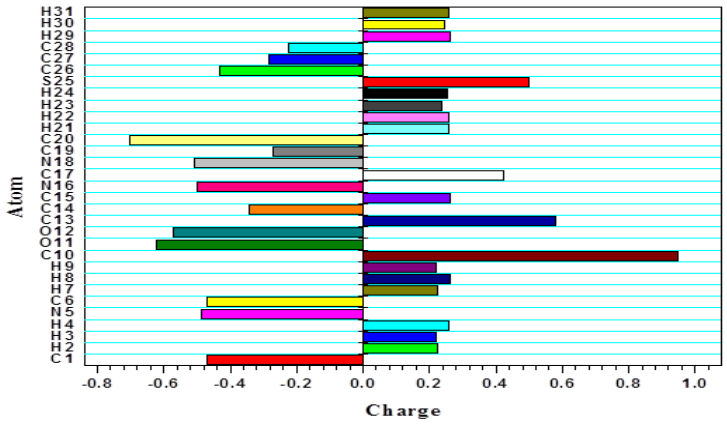

Fig 4: Charge analysis of MTPD

The compound shows that the presence of two large electronegative atom and one nitrogen atom impose very high charge on carbon atom (C_{10}) of the carbamate group. Charge of N_{18} is decreased by the influence of C_{25}-H_{26}…N_{18} hyperconjugative interaction. It is worthy to mention that C_{10}, C_{13}, C_{17} and C_{15} atoms exhibit positive charge while other carbon atoms exhibit negative charge. C_{20} having maximum negative value because of the attached electron donating methyl group. The charge on H_8 in methyl group shows the maximum magnitude of 0.264e among the hydrogen atom due to the C_6-H_8…O_{11} hydrogen bonding interaction.

3.6. Vibrational Analysis

The MTPD has 31 atoms with 87 modes of vibrations. The molecule does not exhibit symmetry and hence belongs to the C_1 point group. The assignment of MTPD was done by theoretical calculations. The theoretical IR spectrum is shown in fig 5. The detailed vibrational assignments of calculated frequencies have been reported in the table 3.

Table 3: The detailed vibrational assignments of calculated frequencies of MTPD

Calculated IR wave number	Assignments with PED	IR intensity	Raman intensity
3139	υC27H30(14)+υC26H31(80)	0	0
3126	υC26H31(85)+ υC27H30(12)	0	1
3115	υC14H24(99)	0	1
3099	υC26H31(18)+ υC27H30(73)	1	0
3086	υC1H2(63)+ υC6H7(63)	1	1
3072	υC6H8(92)	0	1
3024	υ_{asy}C20H21(94)	2	25
3001	υ_{asy}C20H21(96)	1	8
2966	υC1H2(21)+ υC6H7(25)+ υC6H9(46)	4	5
2960	υ_{sy}C1H2(71)+ υC6H7(25)	6	4
2942	υ_{sy}C20H21(95)	2	4
2922	υ_{sy}C1H2(10)+ υC6H9(53)	13	8
2915	υ_{sy}C1H2(70)+υC6H9(17)	8	7
1772	υO11C10(77)+ υN5C10(12)	47	1
1568	υC16N15(14)+υN18C13(14)+υC13C14(38)+υN16C15(10)	33	6
1550	υC16N15(34)+υN18C13(34)+βC19C17N16(31)+υC14C15(31)	16	5
1533	υC19C28(54)+υC26C27(54)+υC17C19(11)+ βH29C28C27(12)+βH30H27C26(12)	18	6
1504	βH2C1H3(70)+βH7C6H9(70)	8	11
1473	βH2C1H4(23)+βH2C1H3(24)+ βH7C6H9(24)+βH2C1H3(24)+βH7C6H8(31)	4	57
1469	βH2C1H3(51)+βH7C6H9(51)+βH7C6H8(16)+τH8C6N5C1(11)	4	48
1460	βH2C1H4(57)+βH7C6H8(22)	6	36
1456	βH21C20H22(69)+opC20H2C15H22(14)	9	51
1446	βH21C20H22(84)++opC20H2C15H23(13)	7	5
1434	υC19C28(47)+υC26C27(47)+υC17C19(11)	22	1
1432	βH2C1H4(57)+βH3C1H4(57)+βH8C6H9(17)	20	1
1405	βH8C6H9(51)	6	1
1402	υN1613C15(41)+βH24C14H13(10)	6	3
1392	υN5C10(14)+βH21C20H22(20)	13	2

Continued…

1380	βH21C20H22(38)	8	100
1369	υN16C15(70)+υN18C13(10)+υC17C19(11)+βH21C20H22(27)	11	3
1335	υC16N15(15)+υN18C13(15)+υC13C14(11)+υC14C15(10)	37	4
1324	υC19C28(17)+υC26C27(17)+βH31C26H27(17)	17	1
1243	opC6H7N5H9(10)	8	1
1240	υN16C15(73)+υN18C13(10)	7	0
1209	υC19C28(13)+υC26C27(13)+βH29C28C27(52)+βH30H27C26(52)	3	0
1147	υO12C10(40)+υO12C13(10)+υN5C1(52)+βH24C14H13(37)	17	0
1144	βH7C6H8(10)+opC1H4N5H2(33)+τH8C6N5C1(31)	19	1
1123	υN5C10(12)+ υO12C10(21)+ υO12C13(21)+ βN5C10O11(10)+opC1H4N5H2(33)+opC6H7N5H9(12)+	100	1
1104	υC19C28(10)+υC26C27(10)	17	0
1099	βH7C6H8(10)+opC1H4N5H3(36)+τH8C6N5C1(33)+ βH21C20H22(18)	9	0
1071	υC19C28(13)+υC26C27(13)+βH31C26C27(48)+βH29C28C27(11)	1	0
1052	υN5C1(17)+opC6H7N5H9(31)	2	1
1032	βH21C20H22(13)++opC20H2C15H23(70)	3	2
1027	υC19C28(24)+υC26C27(24)+βH29C28C27(11)+βH30H27C26(11)	5	1
1013	υO12C10(22)+υO12C13(22)+υN5C1(12)+υN5C6(12)	6	1
990	υC14C15(10)+βC14C13N18(10)+opC20H2C15H22(41)	1	0
964	υN16C15(10)+υN18C13(10)+ βC14C13N18(15)++opC20H2C15H22(13)	0	2
945	υO12C10(20)+υO12C13(20)+υC15C20(10)+ υN5C1(26)+υN5C6(26)	1	5
893	τH29C28C19C17(81)+βH29C28C27(79)	0	0
849	βC17C19C28(26)+opC14C13C15H24(17)	1	0
841	βC17C19C28(33)+opC14C13C15H24(23)	3	0
832	τH29C28C27C26(84)+τH31C26S25C19(84)	1	0
816	βC17C19N28(34)+opC14C13C15H24(15)	4	0
799	υN5C1(10)+υN5C6(10)+opC14C13C15H24(35)	2	0
770	τC15N6C17CN18(58)+τC15C4C13N18(18)	2	1
723	υS25C19(41)+βC17C19C28(42)	1	1
715	opO11N5O12C10(69)	1	1
694	τH29C28C27C26(86)	6	1
672	τC15C4C13N18(18)+opO11N5O12C10(19)+ τC17N18C13O12(12)	2	0
635	βN5C10O12(12)+βC19S25C26(31)	1	2
629	βN16C17N18(12)+βC19S25C26(29)	1	1
599	βN5C10O11(24)+τC15N16C17N16(10)	1	0
569	τC19C28C27C26(11)++τC15N16C17N16(30)	0	0
551	τC19C28C27C26(71)	0	0
534	υC15C20(15)+βC13N18C17(42)	1	0
508	βC13N18C17(11)+βN5C10O12(12)+βC14C13O12(19)+ βC10O12O13(19)+βC14C15C20(11)	0	0

Continued…

457	τC19S25C26C27(80)	0	0
431	υO12C10(10)+υO12C13(10)+βC1N5C10(52)	1	0
368	βC6N5C10(43)	2	0
342	υC17C19(13)+βN16C17N18(12)+βC14C15C20(14)+ βC6N5C10(11)	0	0
329	βC19C17N16(10)+βC17C19C28(42)+βC14C13O12(19)+ βC10O12O13(19)+βC6N5C10(16)	0	0
272	υC17C19(14)	0	0
248	τC17N6C17CN18(58)++τC15N16C17N16(11)	0	0
231	τC17C19S25C26(19)+τC17C19S25C26(14)+ τC15C4C13N18(14)+τC15N16C17C19(12)	0	0
221	opC6C1C10N5(63)	0	0
214	βN5C10O12(12)+βC14C15C20(14)+opC6C1C10N5(11)	0	0
178	τC13C4C15C20(48)	0	0
143	τH4C1N5C6(43)+τC1N5C10O12(18)	0	0
127	τH4C1N5C6(37)	0	0
96	βC17C17N16(13)+τC17C19S25C26(22)+ τC15N16C17C19(31)	0	0
94	τC1N5C10O12(41)+opC6C1C10N5(10)	0	0
70	τH4C1N5C10(70)	0	0
65	τC20H21C5N16(47)	0	0
58	τC20H21C5N16(43)	0	0
47	τC17N18C13O12(17)	0	0
30	τC13O12C10N5(40)+τC1N5C10O12(11)	0	0
21	τC13O12C10N5(50)	0	0

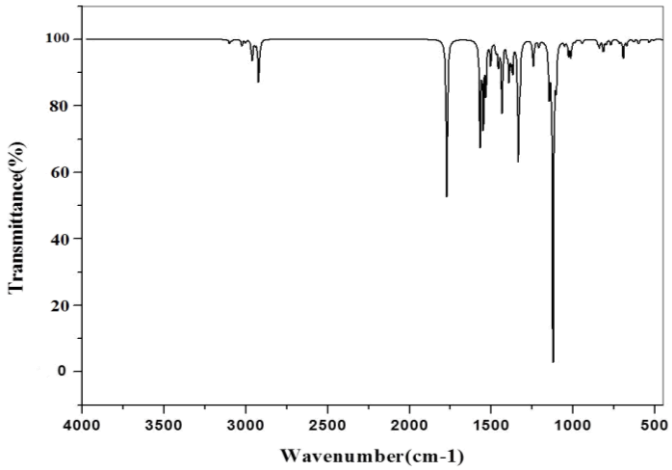

Fig. 5: Theoretical IR spectrum of MTPD

3.6.1. Pyrimidine ring vibration

Spectral region around 3100-3000 cm^{-1} [9] is the characteristic region of C-H vibrations in the heteroatomic structure. However, in tri-substituted pyrimidine with only one free ring hydrogen atom and the band is very weak which is observed at 3115 cm^{-1}. Due to C-C and C-N stretching vibrations, strong absorption in pyrimidine was observed at 1600-1500 cm^{-1}. The fundamental bands due to the coupled C-C and C-N stretching vibrations of pyrimidine ring moiety in TMPD have been observed at 1568 cm^{-1}. Another significant mode to discuss is the ring breathing mode, a distinctive mode for cyclic molecules that is recognized as a powerful band at 964 cm^{-1}. In this regard, this assignment is consistent with different derivatives of pyrimidine. [10–14]. Usually an in plane deformation vibration is at higher than the out of plane vibration. In the present study, the bands observed at 620 cm^{-1} is attributed to ring in-plane bending modes. The ring out-of-plane bending mode is established at 508cm^{-1}.

3.6.2. Thiophene ring vibration

The CH stretching vibrations are expected to appear in the region 3100– 3000 cm^{-1}, with multiple weak bands.

The nature of substituents does not have much effect on the bands in this region [15, 16]. CH stretching vibrations of the molecule is observed at 3099 cm^{-1}. The CH in-plane bendings vibrations appear as sharp but weak to medium bands in the region 1100–1500 cm^{-1}region. The in plane bending mode is observed at 1027 cm^{-1}. These bands are not sensitive to the nature of substituents. The out of plane bending vibrations occur in the wavenumber range 800-1000 cm^{-1}. In TMPD, the out of plane bending mode is observed at 816 cm^{-1}. It is difficult to distinguish the C-S bands in thiophene. This can be clarified by the shorter bond duration and greater polarity of the thiophene C-S bond. [17]. The C-S stretching mode is predicted to occur at 691, 707 $cm^{-1}$and is observed at 743 and 771 cm^{-1} [18].

3.6.3. C=O vibrations

The stretching vibrations of C = O are generally found in the region 1850–1600 cm^{-1} region [19, 20]. In TMPD, the C=O vibrations is observed as very strong band at 1770 cm^{-1}.

3.6.4. Methyl group vibration

For the assignment of CH_3 group frequencies, basically nine fundamentals can be associated to CH_3 group, namely symmetric stretch; asymmetric stretch , in-plane bending, symmetric bending, in-plane rocking, out-of-plane rocking and twisting hydrogen bending modes. In addition to that, out-of-plane stretch, and, out-of-plane bending, modes of the CH_3 group would be expected. The asymmetric stretching wave number is assigned at 3024, 3001$cm^{-1}$and symmetric stretching established at 2942 cm^{-1}. We have observed the symmetrical methyl deformation mode at 1369 cm^{-1}. The methyl in-plane-bending and out-of-plane bending deformation modes are observed at 1446 and 1380cm^{-1} respectively. The in-plane and out-of-plane rocking modes of TMPD observed at 1032 and 1099cm^{-1}. The calculated frequency 65cm^{-1} is attributed to methyl twisting mode.

3.6.5. $(N\text{-}CH_3)_2$ vibration

The CH_3 groups next to the nitrogen atom in amines are somewhat shifted. The symmetric stretch at 2830-2770 cm^{-1} is lowered in wave number and intensified and to stands out among other aliphatic bonds. Due to the possibility of C-H…O hydrogen bonding (C_1-H_4…O_{12} and C_6-H_8…O_{11}) there is a blue shift affected in the region 2915-2966 cm^{-1}. C–N vibrations usually absorb in the region 1350–1160 cm^{-1} [21]. In TMPD these vibrations are observed at 1354cm^{-1},1153cm^{-1} in FTIR and the corresponding calculated values observed at 1169, 1147 cm^{-1} PED percentages of about 70%, 40%.

3.7. HOMO LUMO Analysis

Highest Molecular orbital and Lower Molecular Orbital are very important parameter in quantum chemistry and these orbitals are known as FMO. HOMO can be considered as the outermost orbital which contains electrons representing the ability to donate electron while LUMO can considered the innermost orbital containing few places representing the ability to accept the electrons. The lower value of HOMO-LUMO value indicates both the intra molecular charge transfer within the molecule and lower chemical reactivity. The lower energy gap ($\Delta E=E_{LUMO}-E_{HOMO}$) explains eventual charge transfer within the molecule.

From the energy gap value it is observed that MTPD has lower band energy. It explains an eventual charge transfer interaction within the molecule and high chemical reactivity. The small value of H-L gap gives more number of charge transitions to occur between the thiophene ring to carbamate group through pyrimidine ring that can be effectively used for insecticidal activity [22]. According to calculation, the energy band (ΔE) of the molecule to the first excited state is

HOMO energy: -5.96 eV

LUMO energy: -1.37 eV

HOMO-LUMO energy gap: 4.59 eV

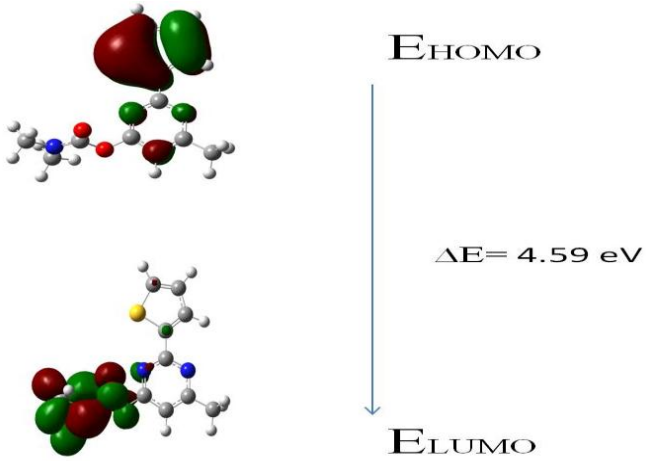

Fig. 6: HOMO and LUMO plot of MTPD

The HOMO LUMO energy gap explains the eventual charge transfer interaction taking place within the molecule. The frontier orbital (HOMO, LUMO) of MTPD is plotted in Fig.6.

By using HOMO and LUMO energy values for a molecule, electronegativity and chemical hardness can be calculated as follows:

Global reactivity descriptors are calculated using the energies of frontier molecular orbitals E_{LUMO} as $\chi = 1/2(E_{HOMO}+E_{LUMO})$, $\mu = -1/2\ (E_{HOMO}+E_{LUMO})$, $\eta = 1/2(E_{HOMO} - E_{LUMO})$, $S=1/2\eta$ and $\omega = \mu^2/2\eta$. The energies of frontier molecular orbitals (E_{LUMO}, E_{HOMO}) and global reactivity descriptors are listed in table 4. Energy gap of title molecule is calculated 4.590eV. A molecule with a small frontier orbital gap is generally associated with a high chemical reactivity and low kinetic stability. Larger the HOMO-LUMO energy gap, harder the molecule. Higher the value of the electrophilicity index better is the electrophilic character. The Zero point vibrational Energy, Dipole moment (D) and SCF Energy are calculated as 629.27kJ/mol, 2.822 and -1178.018 respectively.

Table 4: Global reactivity descriptors

Global reactivity descriptors	MTPD
Ionization potential (I)	5.960
Electron affinity (A)	1.370
Electro-negativity (χ)	3.665
Chemical potential (μ)	-3.665
Global hardness(η)	2.295
Global softness (S)	0.218
Electrophilicity index (ω)	2.926

3.8. Local reactivity descriptors

The Fukui function is a descriptor of local reactivity that shows the preferred regions where a chemical species will change its density when the number of electrons is modified. The Fukui function is a local reactivity descriptor that indicates the preferred areas where a chemical species changes its density when the number of electrons changes. The condensed or atomic Fukui functions on the j^{th} atom site are given as per the following equations for an electrophilic $f_j^-(r)$, nucleophilic and free radical attack $f_j^+(r)$, on the reference molecule, respectively listed in table ().

$f_j^- = q_j(N) - q_j(N-1)$

$f_j^+ = q_j(N+1) - q_j(N)$

$f j^0 = 1/2\ [q_j(N+1) - q_j(N-1)]$

Morell et al. [23] proposed a dual descriptor ($\Delta f(r)$), defined as the difference between the nucleophilic and electrophilic Fukui function and is given by:

$$\Delta f(r) = [f^+(r) - f^-(r)]$$

If $\Delta f(r) > 0$, the site is favoured for a nucleophilic attack. If $\Delta f(r) < 0$, the site may be favoured for an electrophilic attack. Dual descriptors $\Delta f(r)$ gives a clear difference between nucleophilic and electrophilic attack at a particular region with their sign. It gives positive value for site where nucleophilic attack is possible and a negative value where electrophilic attack is possible.

Table 5: Condensed fukui function of FC molecule by UCA-FUKUI

Atoms	f^-	f^+	f^0	dual descriptor Δf
C1	-0.0108	-0.0046	0.0077	-0.006
H2	0.0234	0.0117	0.0175	-0.012
H3	0.0265	0.0167	0.0216	-0.0099
H4	0.0023	-0.0075	0.0026	0.0050
N5	0.0717	0.0104	0.041	-0.061
C6	-0.0105	-0.0047	0.0076	-0.006
H7	0.0217	0.0100	0.0158	-0.012
H8	0.0077	0.0027	0.0052	-0.005
H9	0.0264	0.0159	0.0211	-0.010
C10	-0.0099	-0.0073	0.0086	-0.003
O11	0.0453	0.0059	0.0256	-0.039
O12	0.0198	0.0119	0.0159	-0.008
C13	0.0048	0.0272	0.0160	0.0220
C14	0.1101	0.1235	0.1168	0.014
C15	0.0117	0.0337	0.0227	0.022
N16	0.0547	0.0382	0.0464	-0.017
C17	-0.017	0.1162	0.0496	0.099
N18	0.032	0.0446	0.0383	0.013
C19	0.121	0.0024	0.0617	-0.119
C20	-0.0126	-0.015	0.0138	0.002
H21	0.0196	0.0225	0.021	0.003
H22	0.0196	0.0229	0.0213	0.003
H23	0.0179	0.023	0.0205	0.005
C24	0.0264	0.0389	0.0327	0.013
S25	0.0667	0.1373	0.1020	0.0710
C26	0.1367	0.0981	0.1174	-0.039
C27	0.0433	0.0106	0.0270	-0.033
C28	0.0535	0.1065	0.0800	0.0530
H29	0.0293	0.0297	0.0295	0.0004
H30	0.0364	0.0383	0.0373	0.0020
H31	0.0325	0.0404	0.0365	0.0080

From the values reported in table 5 the nucleophillic attacking sites for the title compound are H_4, C_{13}, C_{14},

C_{15}, N_{18}, C_{20}, H_{21}, H_{22}, H_{23},C_{24}, S_{25}, C_{28}, H_{29}, H_{30}, H_{31}(positive value i.e. $\Delta f(r)>0$) and the electrophillic attacking sites are C_1, H_2, H_3, N_5, C_6, H_7, H_8, H_9, C_{10}, O_{11} ,O_{12}, N_{16}, C_{19}, C_{26}, C_{27}.(negative value i.e. $\Delta f(r) < 0$).

3.9. Molecular docking

The Docking study of MTPD was performed with two different proteins. Docking is performed for the different receptors (PDB ID-1JI6, 1DLC) and shown in table 6; autodock binding energies, binding residues and bond energy were obtained. Among them the inhibition of MTPD with 1DLC target protein has the lowest free energy -6.20 kcal/mol. Thus this possesses the highest potential binding affinity into the binding site of the molecule. Out of hundred docking runs converged on a top-ranked cluster (1DLC) as shown in Fig. 7, the best docked conformations are those found to have the lowest binding energy and the greatest number of members in the cluster, indicating good convergence. Carbamate group present in the active site of the target ASN 618 is attached to MTPD by C-H…O hydrogen bonding indicated by dashed lines. From the above observations it is identified that the binding of protein 1DLC with MTPD is more effective and shows more insecticidal activity. The lowest value of hydrogen bonding interaction leads to the insecticidal activity of the compound (1.98 A°).

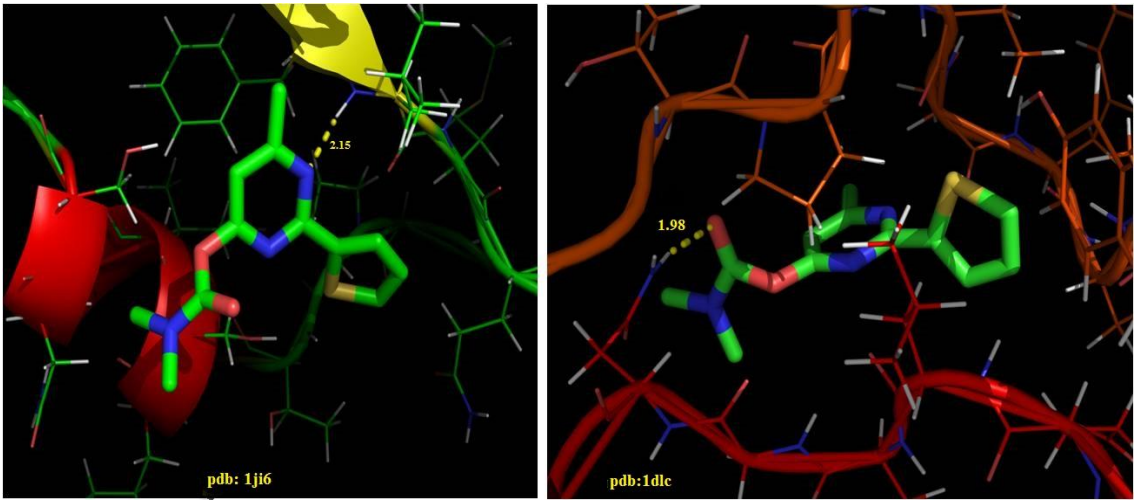

Fig. 7: Autodocked target proteins for MTPD

Table 6: Molecular docking results of MTPD with different protein targets

Protein (PDB:ID)	Binding Residue	Bond energy	H-Bond distance	Incubation constant (µm)	Binding affinity (kcal/mol)
1JI6	LEU 483	-5.29	2.15	321.69	-4.4
1DLC	ASN 618	-7.09	1.98	26.68	-6.2

4. CONCLUSION

In the present work, the optimized geometric parameters (bond lengths, bond angles and dihedral angles) were theoretically determined. The increase in wavenumber from the expected value leads to the blue shift and exhibits the possibility of intramolecular hydrogen bonding. Molecular electrostatic potential shows the carbonyl group having negative potential or donor nature. This gives the evidence for the possibility of C-H…O hydrogen bonding. Fukui function analysis reveals that C_{13} in the pyrimidine ring shows high neucleophilic character. The lowering of HOMO-LUMO band gap supports insecticidal activity of title compound. The lowest binding energy of protein 1DLC with MTPD is more effective and shows more insecticidal activity. Thus from above studies, it can be concluded that TMPD is a good insecticidal agent and further work can be responsible for biological activity.

5. REFERENCS

1. Sham M Sondhi, Nirupma Singh, Monika Johara, Ashok Kumar. *Bioorganic &Medicinal Chemistry*, 2005; **(13)**:6158-6166.
2. Amir M, Javed SA, Harish Kumar. *Indian J. Pharm. Sci.*, 2007, **69 (3)**:337-343.
3. Abu Baker AA. Ahmed Khames A, Mohamed Gad Elkarem. *J. Heterocyclic Chem.*, 2013, **(50):**42.
4. Amalanathan M, Hubert Joe I, Rastogi VK, *Journal of Molecular Structure.* 2011; **(985)**:48-56.
5. Abdullah Al Sehemi G, Ahmad Irfan, Abdullah Asiri M, Yousry Ahmed Ammar. *Spectrochimica Acta Part A: Molecular and Biomolecular Spectroscopy*, 2012; **(91)**:239-243.
6. Arul Dhas D, Hubert Joe I, Roy SDD. *Spectrochimica Acta Part A: Molecular and Bio molecular Spectroscopy*, 2013; **(108)**:89-99.
7. Arul Dhas D, Hubert Joe I, Roy SDD, Balachandran S. *Spectrochimica Acta Part A.*, 2010; **(77)**:36-44.
8. Ayers P W, Robert Parr G, *J.am.Chem.Soc.,* 2000; **(122)**:2010-2018.
9. Socrates G, Infrared Characteristic Group Frequencies, Wiley, Chichester, 1980.
10. Bahat M, Yurdakul S, *Spectrochim. Acta A.,* 2002; **(58)**:933-939.
11. Milani Nejad F, Stidham HD. *Spectrochimica. Acta A.,* 1975; **(31)**:1433-1453.
12. Buyukmurat Y, Akalin E, Ozel AE, Akyuz*, J. Mol. Struct.,* 1999; **(482-483)**:579-584.
13. Martin J M L, Alsenoy C V, *J. Phys. Chem.,*1996; **(100)**:6973-6983.
14. Pongor G, Fogarasi G, Magdo I, Boggs J E, Keresztury G, Ignatyev I.S., *Spectrochim. Acta A.*, 1992; **(48)**:111-119.
15. Varsayani G, Assignments for vibrational spectra of seven hundred benzene derivatives, vols. 1 and 2, Academic Kiado, Budapest, 1973.
16. Jag M, Organic Spectroscopy-Principles and Applications, 2nd ed., Narosa Publishing House, New Delhi, 2001.
17. Sainz Diaz C I, FranciscoMarquez M, Vivier Bunge A. *Theor. Chem. Acc,.* 2010; **(125)**:83-95.
18. Karabacak M, Cınar M, Kurt M. *J. Mol. Struct.,* 2010; **(968)**:108-114.
19. Socrates G. *Infra-Red and Raman Characteristic Group Frequencies*, 3rd ed.; John Wiley & Sons: Chichester, 2001.
20. Bakalska R I, Delchev V B. *J. Mol. Model.,* 2012; **(18):** 5133.
21. Karabacak M, Kurt M, Ahmet Atac, *J. Phys. Org. Chem.,* 2009; **(22)**:321-330.
22. Prabavathi N, Nilufer A, Krishnakumar V, Akilandeswari L. *Spectrochimica Acta Part A: Molecular and Biomolecular Spectroscopy*., 2012; **(96)**:226-241.
23. Morell C, Grand A, Toro-Labbe A. *J. Phys. Chem. A.*, 2005; **(109)**:205.